Magnetic Ordering and Spin Waves in $Na_{0.82}CoO_2$

S. P. Bayrakci,[1] I. Mirebeau,[2] P. Bourges,[2] Y. Sidis,[2] M. Enderle,[3] J. Mesot,[4] D. P. Chen,[1] C. T. Lin,[1] and B. Keimer[1]

[1]*Max Planck Institute for Solid State Research, Heisenbergstrasse 1, D-70569 Stuttgart, Germany*

[2]*Laboratoire Léon Brillouin, CEA/CNRS, F-91191 Gif-sur-Yvette CEDEX, France*

[3]*Institut Laue-Langevin, 156X, 38042 Grenoble CEDEX 9, France*

[4]*Laboratory for Neutron Scattering, ETH Zurich and Paul Scherrer Institute, 5232 Villigen PSI, Switzerland*

(Received 8 October 2004; published 22 April 2005)

Na_xCoO_2, the parent compound of the recently synthesized superconductor $Na_xCoO_2{:}yH_2O$, exhibits bulk antiferromagnetic order below $\sim$20 K for $0.75 \leq x \leq 0.9$. We have performed neutron scattering experiments in which we observed Bragg reflections corresponding to *A*-type antiferromagnetic order in a $Na_{0.82}CoO_2$ single crystal and characterized the corresponding spin-wave dispersions. The spin waves exhibit a strongly energy-dependent linewidth. The in-plane and out-of-plane exchange constants resulting from a fit to a nearest-neighbor Heisenberg model are similar in magnitude, which is unexpected in view of the layered crystal structure of Na_xCoO_2. Possible implications of these observations are discussed.

DOI: 10.1103/PhysRevLett.94.157205 PACS numbers: 75.30.Ds, 72.80.Ga, 75.25.+z

The cobaltate $Na_xCoO_2{:}yH_2O$ has recently enjoyed intense attention. The composition with $x \sim 0.30$, $y \sim 1.4$ has been shown to be superconducting over a narrow range of x, with maximum transition temperature $T_c \sim 5$ K [1,2]. This compound is particularly interesting because its structure is similar to that of the high-T_c copper oxide superconductors. In both materials, superconducting sheets containing oxygen and a spin-1/2 transition metal are separated by layers of lower conductivity in an anisotropic crystal structure. However, a number of characteristics suggests that the superconductivity in this compound may be unusual in different ways from that found in the cuprates. For example, some experiments indicate that the symmetry of the Cooper pair wave function may be *p* wave [3,4].

The unhydrated parent compound Na_xCoO_2 is interesting in its own right owing to its exceptionally high thermopower over the range $0.5 \leq x \leq 0.9$, which, unusually, accompanies low resistivity and low thermal conductivity [5,6]. Magnetic susceptibility data for compounds with $0.5 \leq x \leq 0.7$ show Curie-Weiss behavior with a negative Weiss temperature [7–9]. No static magnetic ordering has been observed for $x \leq 0.7$ in muon spin rotation (μSR) experiments [10]. The magnetism in this system depends sensitively on the doping level: μSR experiments performed on powder samples with $x = 0.75$ suggested the presence of a magnetically ordered phase below $T = 22$ K [11]. Recent magnetic susceptibility measurements have shown evidence of antiferromagnetic (AF) long-range order below 20 K for $0.75 < x < 0.90$ [6,12]. Anisotropic dc magnetic susceptibility and μSR measurements on the $x = 0.82$ composition both showed that the Co spins are oriented along the *c* axis [12]. Searches using unpolarized neutrons for evidence of corresponding static magnetic order have thus far been unsuccessful [13].

In a recent time-of-flight experiment on a Na_xCoO_2 crystal with $x = 0.75$, Boothroyd *et al.* observed ferromagnetic (FM) fluctuations within the *ab* planes [13]. However, the *c*-axis momentum transfer could not be varied independently of the energy transfer in this experiment and, correspondingly, only a projection of the scattering cross section onto the *ab* plane was probed. The magnetic ordering pattern below T_N, as well as the exchange parameters and their relationship to the macroscopic susceptibility above T_N, has thus far remained undetermined. These issues are addressed in the neutron scattering studies reported here. For single crystals with $x = 0.82$, we find static ordering and low-energy fluctuations characteristic of *A*-type antiferromagnetism, namely, antiferromagnetically coupled ferromagnetic layers. Surprisingly, the AF interlayer exchange constant resulting from a fit to a simple Heisenberg model is almost as large as the intralayer FM exchange, despite the difference in Co-Co distances. A possible relationship of this observation to the Co^{3+}-Co^{4+} charge-ordered states recently suggested on the basis of NMR [14,15] and optical conductivity [16] experiments is discussed.

Single crystals of γ-phase Na_xCoO_2 were grown by the floating-zone technique in an image furnace [12,17]. The sodium and cobalt contents were determined through analysis of pieces cut from the same ingots and adjacent to the crystals used for the neutron scattering experiments, using inductively coupled plasma atomic emission spectroscopy and atomic absorption spectroscopy. The Na:Co ratio was found to be $x = 0.82 \pm 0.04$ for each of the two crystals examined in this experiment. Magnetic susceptibility measurements were performed on portions of the ingots adjacent to the crystals used in the experiment. All of the pieces tested exhibited the expected AF transition at $\sim$20 K [12].

We discuss first the determination of the magnetic ordering pattern by elastic neutron scattering. We used the polarized-beam spectrometer 4F1 at the Laboratoire Léon Brillouin, Saclay, France, to monitor the neutron scattering intensity in the spin-flip (SF) and non-spin-flip (NSF) channels at a number of high-symmetry points in the reciprocal lattice. Figure 1 shows the SF intensity (normalized to the NSF intensity) at the (100) and (101) reciprocal-lattice vectors [18] as a function of temperature, with the neutron polarization $\mathbf{P} \parallel \mathbf{Q}$. Temperature-independent contributions to the intensity are present at both positions. These contributions originate mostly from the leakage of NSF scattering from the corresponding nuclear Bragg reflections (which are not forbidden at these reciprocal-lattice vectors), due to the usual limitations of the instrument. For $\mathbf{Q} = (101)$, an additional contribution to the SF intensity originating from electronic magnetic scattering appears below T_N. We also observed magnetic intensity below T_N at (103), (105), (111), and (113), whereas none was observed at (100) (see Fig. 1) or (102), within experimental error. This indicates that the magnetic propagation vector is (001). The unit cell of γ-phase Na_xCoO_2 contains two planes of CoO_6 octahedra; a magnetic ordering vector of (001) therefore corresponds to AF ordering in the c direction, combined with FM order within the ab planes (Fig. 1, inset). The dependence of the SF intensity on the neutron spin direction at the sample confirms the inference from the uniform susceptibility of the c-axis orientation of the magnetic moment [12]. The (001) Bragg reflection is unobservable because the spin orientation factor in the elastic neutron scattering cross section vanishes for moments directed along c. By comparing the magnetic intensity at (101) with the nuclear intensity [20] at (100), using the isotropic form factor, we extracted a value of $0.13 \pm 0.02\ \mu_B$ per Co.

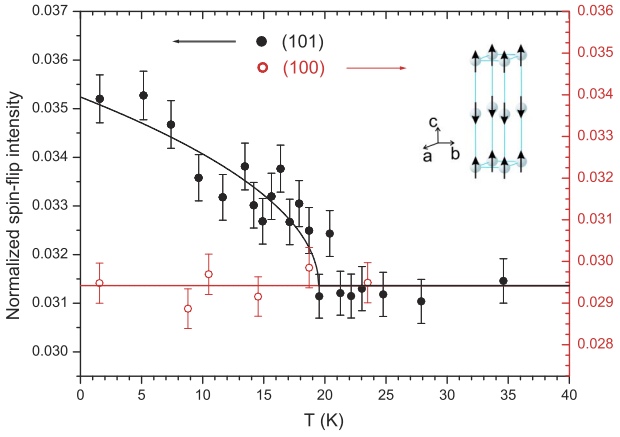

FIG. 1 (color online). Normalized SF intensity (equal to the SF intensity divided by the NSF intensity, viz., the inverse of the flipping ratio as it is usually defined; see text) at $\mathbf{Q} = (101)$ and (100), as a function of temperature. The data were taken with the neutron polarization $\mathbf{P} \parallel \mathbf{Q}$, with $k_i = 2.662$ Å^{-1}. The lines are a guide for the eye. Inset: the A-type AF structure, shown with Co spins $\parallel c$.

The inelastic experiment was performed on the spectrometer IN20 at the Institut Laue-Langevin, Grenoble, France. We used an unpolarized configuration with a double-variable-focusing Si(111) monochromator and a PG(002) analyzer with fixed vertical and horizontal focusing. In order to maximize the flux for the relatively small samples, which had volumes of 147 and 162 mm^3, no collimation was employed. Most of the data were taken with either a fixed final neutron wave vector of $k_f = 2.662$ Å^{-1} or a fixed incident wave vector of $k_i = 4.1$ Å^{-1}. The full width at half maximum (FWHM) of the energy resolution at zero energy transfer is approximately 1 meV in the former arrangement and 3 meV in the latter. The samples were each mounted in the (HHL) scattering plane and placed in a pumped ^{4}He cryostat.

Low-temperature scans at constant-energy transfer $\hbar\omega$ through the ordering wave vector (001) along the in-plane $(hh0)$ direction are shown in Fig. 2. Since the instrumental resolution width is narrow relative to the peak widths, especially at large energy transfers, the data shown were fitted to unconvoluted Lorentzians. As a consequence of the large peak widths at higher excitation energies, interference from an optical phonon at $\hbar\omega = 20$ meV, and the lower neutron flux at larger incident energies, it was not possible in this experiment to determine the dispersion relation up to the in-plane magnetic zone boundary. The inset shows similar scans taken with energy transfer $\hbar\omega = 5$ meV at 1.6 and 100 K, with coarser instrumental resolution ($k_i = 4.1$ Å^{-1}). The integrated intensity decreases

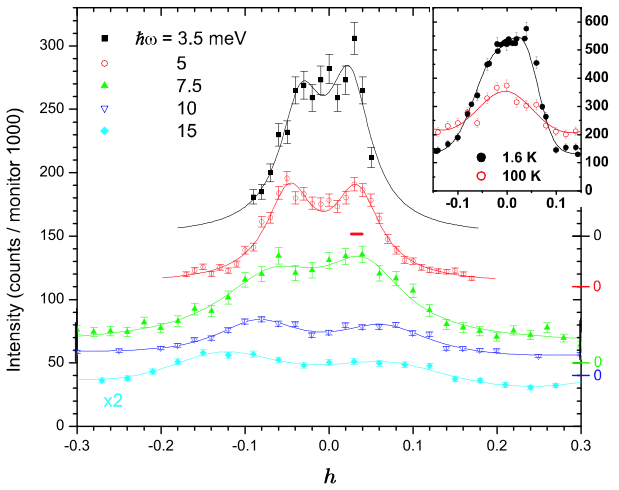

FIG. 2 (color online). Scans at constant-energy transfer $\hbar\omega$ taken along the $(hh0)$ direction through (001) (for $\hbar\omega \leq 5$ meV) or (003), at 1.6 K. The fits are to double Lorentzians. The red bar indicates an estimate of the FWHM of the instrumental resolution for the scan at $\hbar\omega = 5$ meV. For clarity, the data have been offset vertically for the scans with $\hbar\omega < 15$ meV (the corresponding vertical-axis zeros are indicated at right) and the 15 meV data have been scaled by a factor of 2. Inset: constant-energy scans along $(hh0)$ through (001) at energy transfer of 5 meV, at 1.6 and 100 K. The fits are to double Gaussians. The axis units are the same as in the main panel.

with increasing temperature, characteristic of a magnetic excitation. The separation between the two peaks is indistinguishable from zero at 100 K, which suggests that this signal arises from overdamped low-dimensional fluctuations. Comparison of this low-temperature scan through (001) with an equivalent one through (003) (not shown) demonstrates that the intensity decreases with increasing $|\mathbf{Q}|$, as expected for a magnetic excitation. No magnetic intensity was detected in similar scans through (002) and (004).

For out-of-plane wave vectors, the magnon dispersion could be mapped out over the entire magnetic Brillouin zone. A set of constant-$\mathbf{Q}$ scans is shown in Fig. 3. The curves show results of a convolution of the full 3D magnon dispersion scattering with the instrumental resolution, assuming a Lorentzian line shape. Consideration of the fully convoluted dispersion was necessary for accurate determination of the peak positions because of the steep dispersion of the magnon branches in the orthogonal $(hh0)$ direction. In data taken at 50 K ($\sim 2.5T_N$), the magnons are no longer present.

The dispersion data in both directions are summarized in Fig. 4. Assuming nearest-neighbor interactions only, the spin Hamiltonian of an A-type antiferromagnet with localized spins can be written as

$$H = J_{\parallel} \sum_{\substack{i,j \\ \text{in plane}}} \mathbf{S_i} \cdot \mathbf{S_j} + J_{\perp} \sum_{\substack{i,j \\ \perp\text{plane}}} \mathbf{S_i} \cdot \mathbf{S_j} - D \sum_i S_i^z, \quad (1)$$

where $\mathbf{S_i}$ is the spin-1/2 operator for the magnetic ion at lattice site i and the coupling constants $J_{\parallel}$ and $J_{\perp}$ characterize the exchange interactions within the ab plane and between adjacent planes, respectively. The anisotropy constant D, the sign of which alternates from layer to layer, models the exchange anisotropy; it quantifies the tendency of the spins to align along the c axis. The magnon dispersion can be calculated using the Holstein-Primakoff formalism [20]; the resulting spin-wave dispersion expression for $\mathbf{q} = (hkl)$ is

$$\hbar\omega = 2S\sqrt{\{J_{\perp}(0) - [J_{\parallel}(0) - J_{\parallel}(\mathbf{q})] + (D/2S)\}^2 - \{J_{\perp}(\mathbf{q})\}^2}, \quad (2)$$

where $J_{\parallel}(\mathbf{q}) = 2J_{\parallel}\{\cos(2\pi h) + \cos(2\pi k) + \cos[2\pi(h + k)]\}$ and $J_{\perp}(\mathbf{q}) = 2J_{\perp}\cos(\pi l)$. We fitted the dispersion data in the $(hh0)$ and $(00l)$ directions simultaneously and extracted the following values: $J_{\parallel} = -4.5 \pm 0.3$ meV, $J_{\perp} = 3.3 \pm 0.3$ meV, and $|D| = 0.05 \pm 0.05$ meV. Given the error in the peak position associated with the energy scan through the zone center at (003), and the large error in the fitted value of the anisotropy parameter, the question of whether there is an excitation gap at the AF zone center cannot be answered definitively by our data, and awaits further experiments using cold neutrons. Because of the dilution of spin-1/2 sites assumed for $x = 0.82$, the above calculation is only quantitatively accurate if the material is phase-separated into magnetically ordered regions with a dense network of spin-1/2 sites and nonmagnetic regions. Another scenario, in which the spin-1/2 sites form an ordered superlattice, is discussed below. However, if the charge is uniformly distributed in the CoO_2 layers or exhibits a small modulation in density, the calculation should be repeated using an itinerant model.

Several aspects of our data are surprising. First, the spin-wave dispersion along the ab plane is considerably steeper

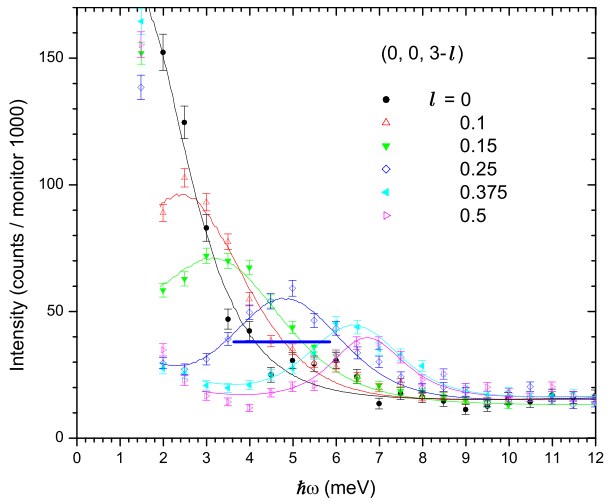

FIG. 3 (color online). Constant-$\mathbf{Q}$ scans taken at different values of $(0, 0, 3 - l)$, with $T = 1.6$ K and $k_f = 2.662$ Å^{-1}. The curves are the results of convolutions of the full spin-wave dispersion (see Fig. 4) with the instrumental resolution ellipsoid; the blue bar indicates an estimate of the FWHM of the instrumental resolution for the scan with $l = 0.25$.

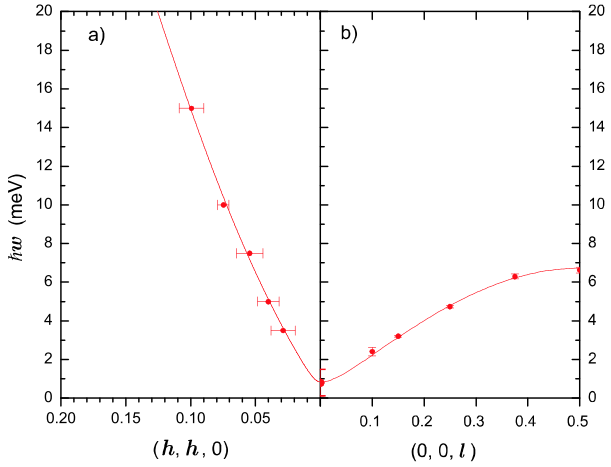

FIG. 4 (color online). (a) Spin-wave dispersion along $(hh0)$; the peak positions are from Fig. 2. (b) Dispersion along $(00l)$, with peak positions from Fig. 3. All data were taken at 1.6 K. The dispersion curves are the result of a fit to the model described in the text.

than that along the c direction, but the magnon bandwidth is proportional to the number of nearest neighbors, which is six within the ab plane and only two along c. Hence, $J_{\parallel}$ and $J_{\perp}$ are in fact comparable in magnitude. This relative isotropy is surprising in light of the two dimensionality of the Na_xCoO_2 crystal structure. In other layered magnets with comparable bond-length anisotropies, such as $YBa_2Cu_3O_6$, the magnitudes of the in-plane and out-of-plane exchange parameters differ by orders of magnitude [21]. It is also surprising that the Curie-Weiss temperature inferred from the fitted exchange parameters in the context of a local-moment picture, $-(3J_{\parallel} + J_{\perp})/k_B$, is positive, whereas that extracted from the magnetic susceptibility measurements is negative.

The microscopic origin of these findings should be addressed by theory. Since an unusually strong c-axis superexchange coupling through Na or an unusually weak nearest-neighbor in-plane exchange coupling would explain the isotropy of the spin-wave dispersions, a computation of these quantities is particularly desirable. A recent theoretical study has pointed out the relevance of longer-range exchange interactions along c [22]. Another possible origin of our observation is an in-plane charge-ordered superstructure recently suggested pursuant to NMR [14,15] and optical conductivity [16] experiments. The distribution of cobalt valence states has thus far not been elucidated directly. If all of the Co ions are in low-spin local-moment states (that is, $S = 1/2$ for Co^{4+} and $S = 0$ for Co^{3+}), then for $x = 0.82$ the spin lattice is dilute, with only 18% of the Co sites occupied by $S = 1/2$ spins. One possible arrangement of these spins, achievable exactly for $x = 0.75$, is that of a triangular lattice with lattice constant $2a$. Since this is comparable to the out-of-plane Co-Co distance, isotropic spin-wave dispersions would be a natural consequence. Such a spin ordering could be inferred from more complete measurements of the ab-plane magnon dispersion. A scenario in which the Co^{3+} ions in the superstructure are in an intermediate-spin state with $S = 1$ and interact antiferromagnetically [16] could help explain why the bulk dc susceptibility in $Na_{0.82}CoO_2$ is AF, despite the fact that $-(3J_{\parallel} + J_{\perp}) > 0$.

If the cobalt valence is in fact distributed relatively uniformly, an itinerant-electron picture should be considered instead. In this case, the magnetic ordering would correspond to a spin-density wave.

Another interesting aspect of our results is the q width of the $(hh0)$ magnons, which increases with increasing $|\mathbf{q}|$ (Fig. 2). The large peak widths may reflect short-ranged magnetic correlations within the ab planes. An alternate possibility is Landau damping by charged quasiparticles. In a charge-ordered scenario with antiferromagnetically interacting, intermediate-spin Co^{3+} ions arranged on a geometrically frustrated Kagomé lattice [16], the broadening may also arise from an admixture of excitations from the disordered array of Co^{3+} spins.

In conclusion, our measurements demonstrate that $Na_{0.82}CoO_2$ exhibits spin fluctuations characteristic of low-temperature 3D AF ordering of the A type, with magnetic exchange constants much less anisotropic than expected, given the layered crystal structure [23]. The antiferromagnetism coexists with metallic conductivity. Unanswered questions remain regarding the degree to which the spins have localized or itinerant character, possible superstructure in the former case, and the microscopic character of the exchange couplings. Answers to these questions may also shed light on the origin of the unusual thermal properties of Na_xCoO_2 and on the superconducting state in the hydrated analogue.

We thank C. Bernhard, A. T. Boothroyd, A. Ivanov, G. Khaliullin, R. K. Kremer, J. Kulda, P. Lemmens, I. Mazin, W. Pickett, and R. Zeyher for helpful discussions, and E. Brücher, V. Duppel, and G. Götz for technical assistance.

[1] K. Takada *et al.*, Nature (London) **422**, 53 (2003).
[2] R. E. Schaak *et al.*, Nature (London) **424**, 527 (2003).
[3] W. Higemoto *et al.*, Phys. Rev. B **70**, 134508 (2004).
[4] T. Fujimoto *et al.*, Phys. Rev. Lett. **92**, 047004 (2004).
[5] I. Terasaki *et al.*, Phys. Rev. B **65**, 195106 (2002).
[6] M. Mikami *et al.*, Jpn. J. Appl. Phys. **42**, 7383 (2003).
[7] R. Ray *et al.*, Phys. Rev. B **59**, 9454 (1999).
[8] J. L. Gavilano *et al.*, Phys. Rev. B **69**, 100404 (2004).
[9] Y. Wang *et al.*, Nature (London) **423**, 425 (2003).
[10] J. Sugiyama *et al.*, Phys. Rev. B **66**, 134413 (2002).
[11] J. Sugiyama *et al.*, Phys. Rev. B **67**, 214420 (2003).
[12] S. P. Bayrakci *et al.*, Phys. Rev. B **69**, 100410(R) (2004).
[13] A. T. Boothroyd *et al.*, Phys. Rev. Lett. **92**, 197201 (2004).
[14] F. L. Ning *et al.*, Phys. Rev. Lett. **93**, 237201 (2004).
[15] I. R. Mukhamedshin *et al.*, Phys. Rev. Lett. **93**, 167601 (2004).
[16] C. Bernhard *et al.*, Phys. Rev. Lett. **93**, 167003 (2004).
[17] D. P. Chen *et al.*, Phys. Rev. B **70**, 024506 (2004).
[18] We use a notation in which the momentum $\mathbf{Q}$ transferred by the neutron is $\mathbf{Q} = \mathbf{q} + \boldsymbol{\tau}$, where $\mathbf{q}$ is the momentum transfer within the Brillouin zone centered at the reciprocal-lattice vector $\boldsymbol{\tau}$. These quantities are expressed in reduced lattice units based on the hexagonal space group $P6_3/mmc$, with $a = b \sim 2.84$ Å and $c \sim 10.7$ Å [19]. For instance, $\mathbf{Q} = (HKL)$, with $Q_c = L\frac{2\pi}{c}$, and $\mathbf{q} = (hkl)$, with $q_c = l\frac{2\pi}{c}$.
[19] R. J. Balsys and R. L. Davies, Solid State Ionics **93**, 279 (1996); Q. Huang *et al.*, Phys. Rev. B **70**, 184110 (2004).
[20] S. W. Lovesey, *Theory Of Neutron Scattering from Condensed Matter* (Clarendon Press, Oxford, 1984), Vol. 2.
[21] J. M. Tranquada *et al.*, Phys. Rev. B **40**, 4503 (1989).
[22] M. D. Johannes *et al.*, cond-mat/0412663 [Phys. Rev. B (to be published)].
[23] Similar results were recently obtained by L. M. Helme *et al.*, following Letter, Phys. Rev. Lett. **94**, 157206 (2005).